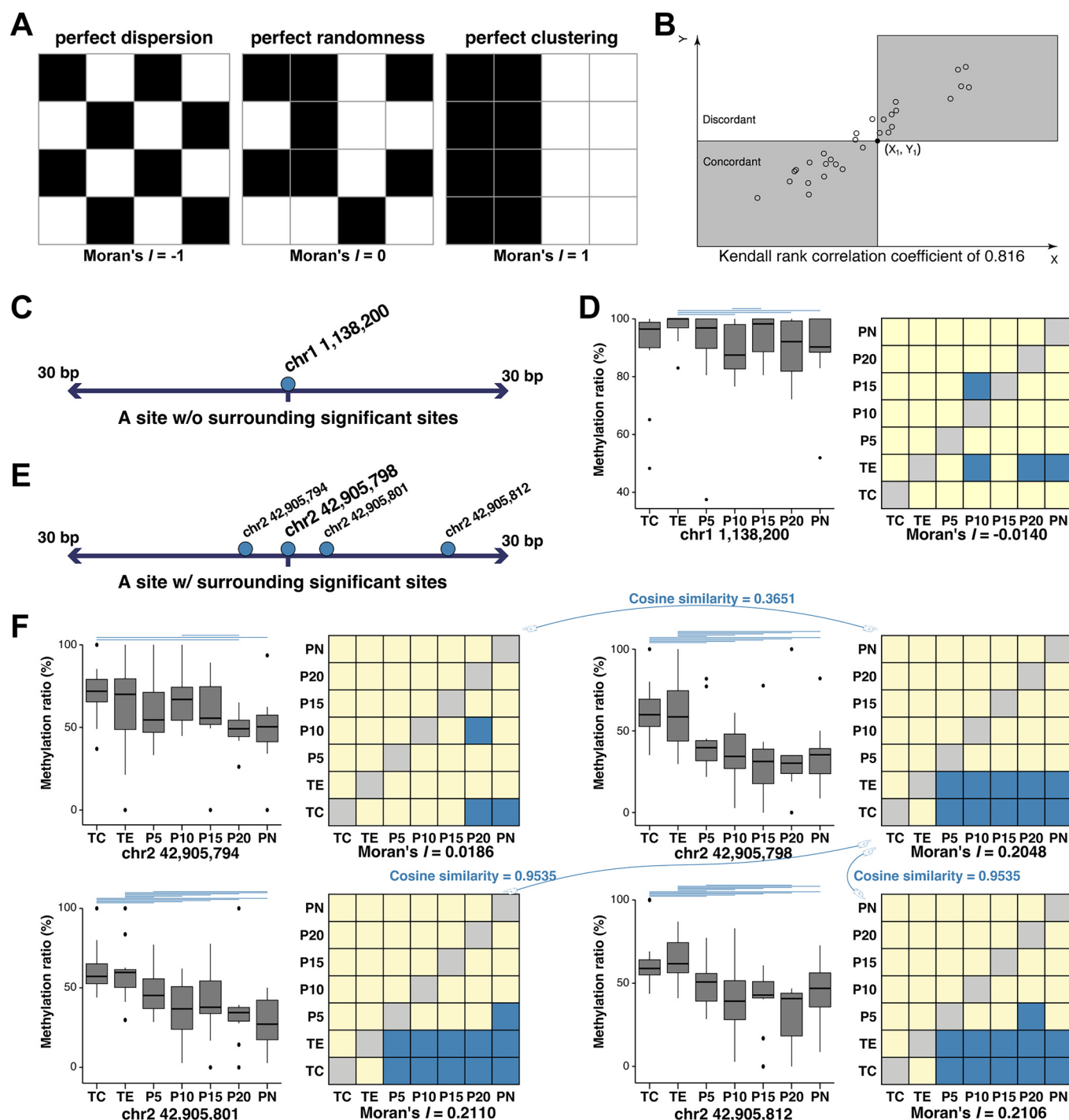
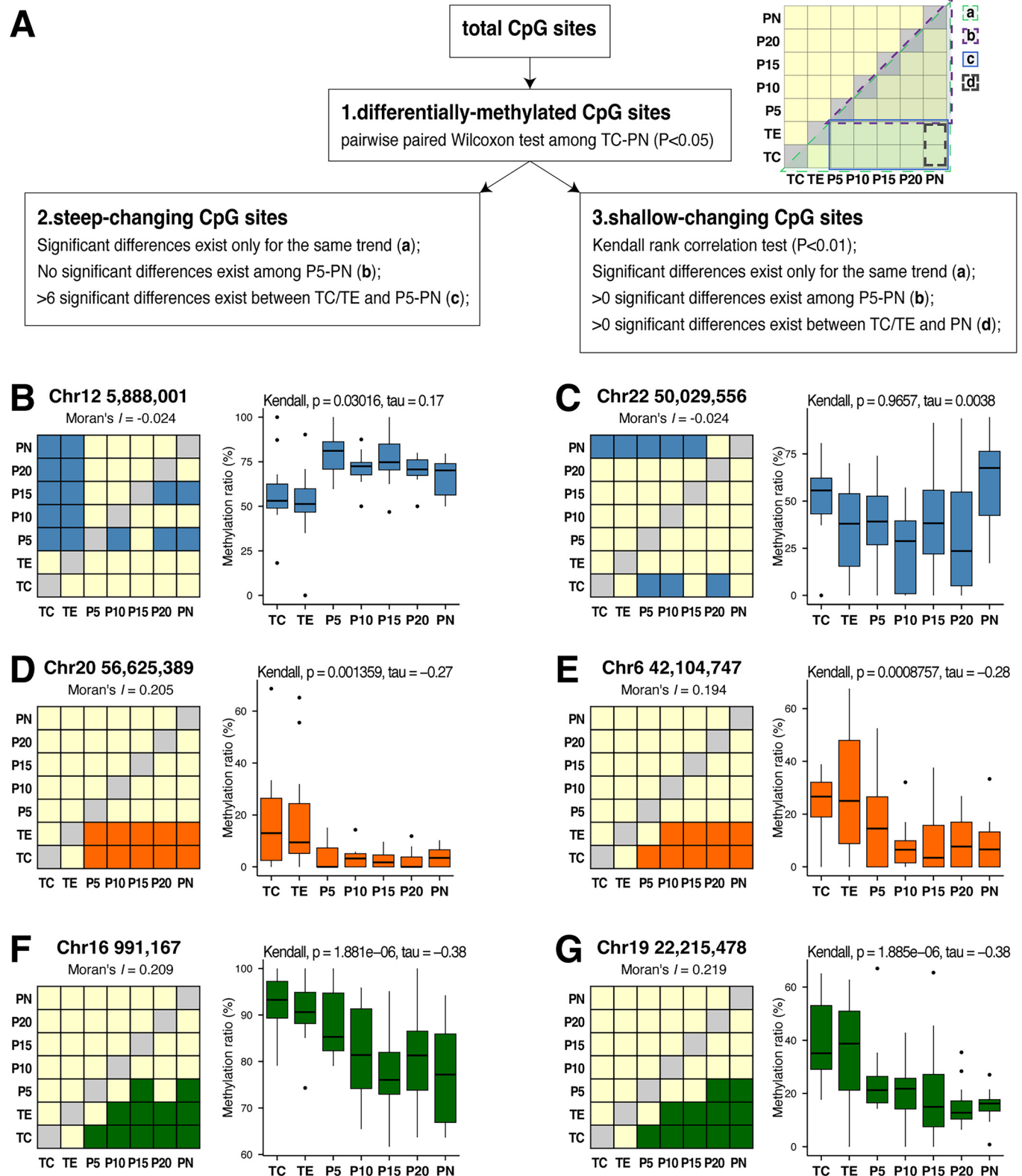


## Expanded View Figures

### Figure EV1. Schematic diagrams illustrating the statistical methods employed.

(A) Illustrations of spatial autocorrelation, featuring three typical distribution examples. (B) Illustration of the Kendall rank correlation coefficient. All points within the gray area are concordant, while those in the white area are discordant to the reference point. This example contains 395 concordant point pairs and 40 discordant pairs, yielding a Kendall rank correlation coefficient of 0.816. (C) The significantly different CpG site at chr1:1,138,200 is associated with no other significant sites within a 30 nt range. (D) Boxplots illustrate the methylation levels of the site chr1:1,138,200 across different locations, while matrices display the significantly associated locations for each CpG site. (E) The significantly different CpG site at chr2:42,905,798 is associated with three other significant sites within a 30 nt range. (F) Boxplots illustrate the methylation levels of these four sites across different locations, while matrices display the significantly associated locations for each CpG site. The methylation patterns of these sites are analogous, with chr2:42,905,798, chr2:42,905,801, and chr2:42,905,812 exhibiting comparable Moran's  $I$  values. The matrices of these three surrounding sites are respectively compared with the calculated cosine similarity of chr2:42,905,798, and the results are shown on the blue lines. Boxplots present with the median as the center, box bounds as the 25th and 75th percentiles, and whiskers extending to the minimum and maximum values within  $1.5 \times \text{IQR}$  ( $n = 12$ ). Outliers beyond  $1.5 \times \text{IQR}$  are plotted as individual points.





**Figure EV2. Classification process for methylation change trends and site examples.**

(A) The screening process and specific criteria for identifying steep- and shallow-changing sites are outlined. Additional details and examples of criteria for judgment can be found in Appendix Methods. (B, C) Two differentially methylated CpG sites were excluded for failing to meet the specified criteria. (D, E) Examples of two steep-changing CpG sites are presented. (F, G) Examples of two shallow-changing CpG sites are presented. Boxplots present with the median as the center, box bounds as the 25th and 75th percentiles, and whiskers extending to the minimum and maximum values within  $1.5 \times \text{IQR}$  ( $n = 12$ ). Outliers beyond  $1.5 \times \text{IQR}$  are plotted as individual points.

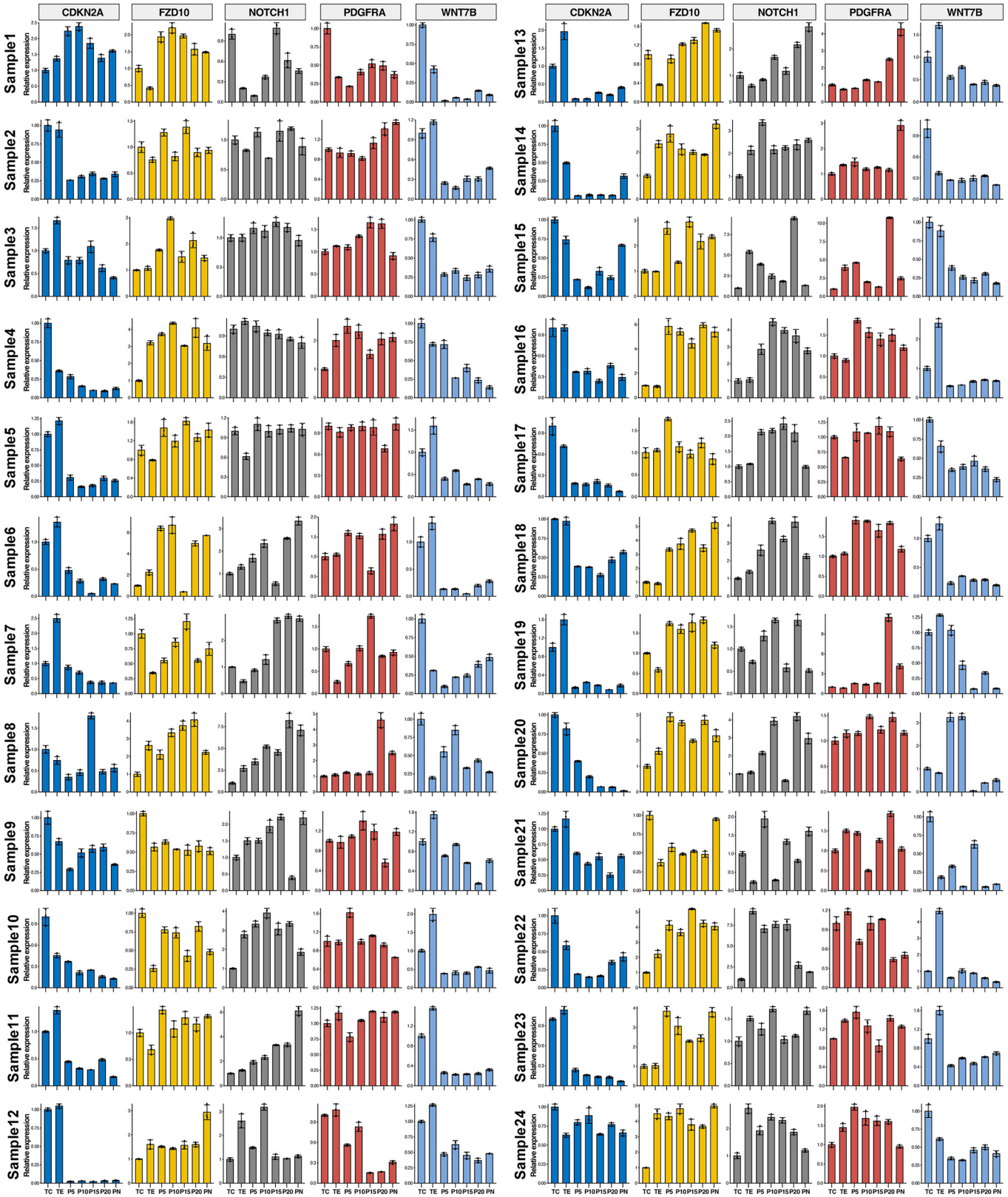
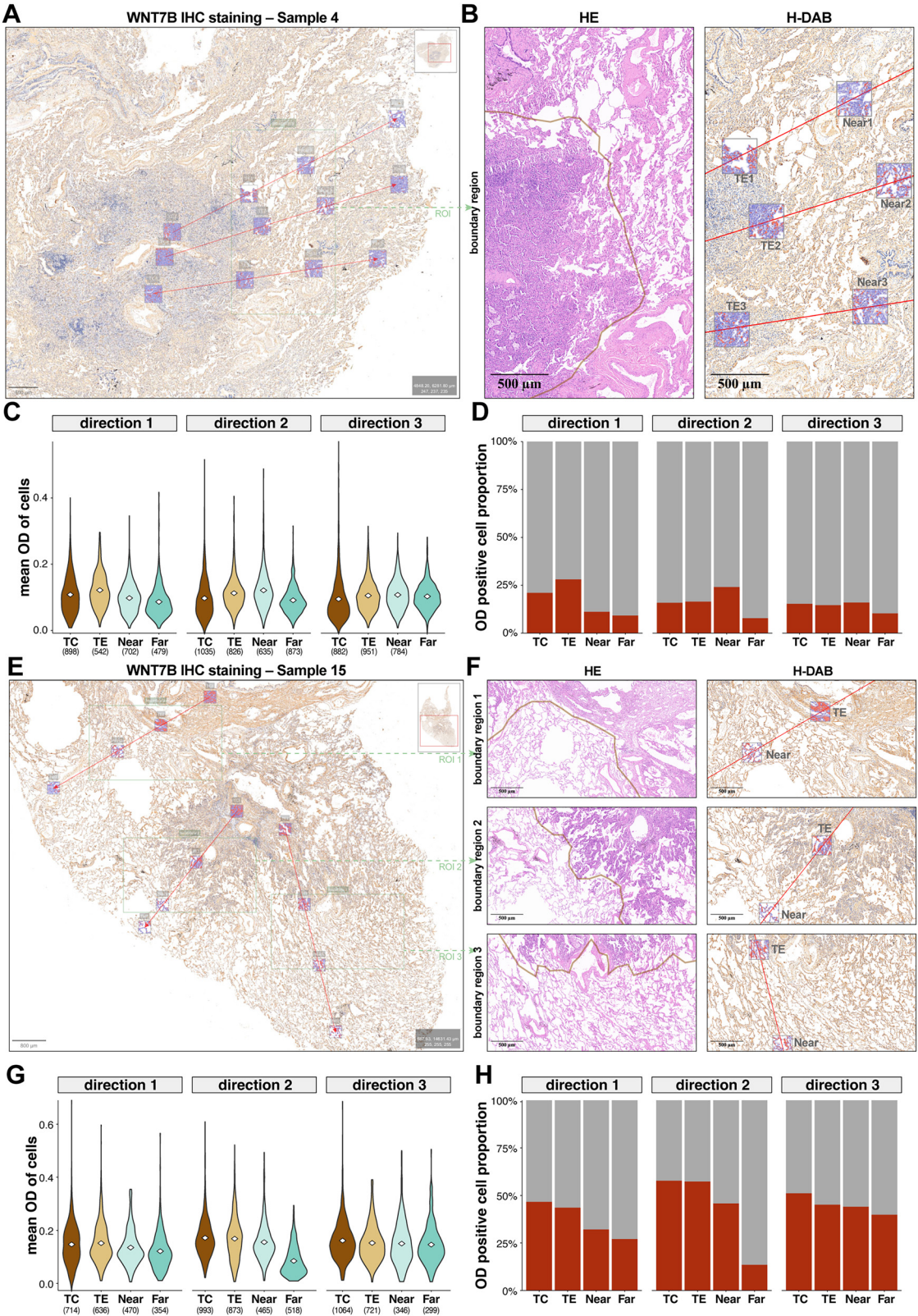


**Figure EV3. Relative gene expression at different locations in each sample measured by RT-qPCR.**

mRNA expression of five genes from 24 patients are presented. Relative expression levels were normalized to the reference gene *ACTB* and standardized to TC's relative expression for comparison, with error bars indicating the mean  $\pm$  standard deviation (SD) from three replicates.



◀ **Figure EV4. WNT7B protein expression profiles of Patient 4 and Patient 15.**

(A) Representative IHC staining of WNT7B protein in LUAD Sample 4. FFPE tumor tissue section was stained using WNT7B antibody. Red lines marked three directions from the tumor core to adjacent tissues, and 300 $\mu$ m-squared regions of interest (ROIs) of the tumor core (TC), tumor edge (TE), and adjacent tissue at different distances (P5-Near and P5-Far) on each direction were selected as for optical density (OD) analysis. (B) A larger ROI covering three pairs of TE and P5-Near regions was selected for the local magnification display of the boundary region in Sample 4. HE and H-DAB staining images showed the visual boundary of the tumor and corresponding DAB signals in TE and P5-Near regions. (C) Violin plots showing the distribution of mean OD per cell for each region (TC, TE, Near, and Far) in three directions of Sample 4 and cell numbers of ROIs were shown below. (D) Proportion of OD-positive cells in each region and direction, based on predefined OD thresholds described in the Methods. (E) Representative IHC staining of WNT7B protein in LUAD Sample 15. FFPE tumor tissue section was stained using WNT7B antibody. Red lines marked three directions from the tumor core to adjacent tissues, and 300 $\mu$ m-squared regions of interest (ROIs) of the tumor core (TC), tumor edge (TE), and adjacent tissue at different distances (P5-Near and P5-Far) on each direction were selected as for optical density (OD) analysis. (F) Three larger ROIs covering the corresponding TE and P5-Near regions were selected for local magnification display of the boundary region in Sample 15. HE and H-DAB staining images showed the visual boundary of the tumor and corresponding DAB signals in TE and P5-Near regions. (G) Violin plots showing the distribution of mean OD per cell for each region (TC, TE, Near, and Far) in three directions of Sample 15 and cell numbers of ROIs were shown below. (H) Proportion of OD-positive cells in each region and direction in Sample 15.

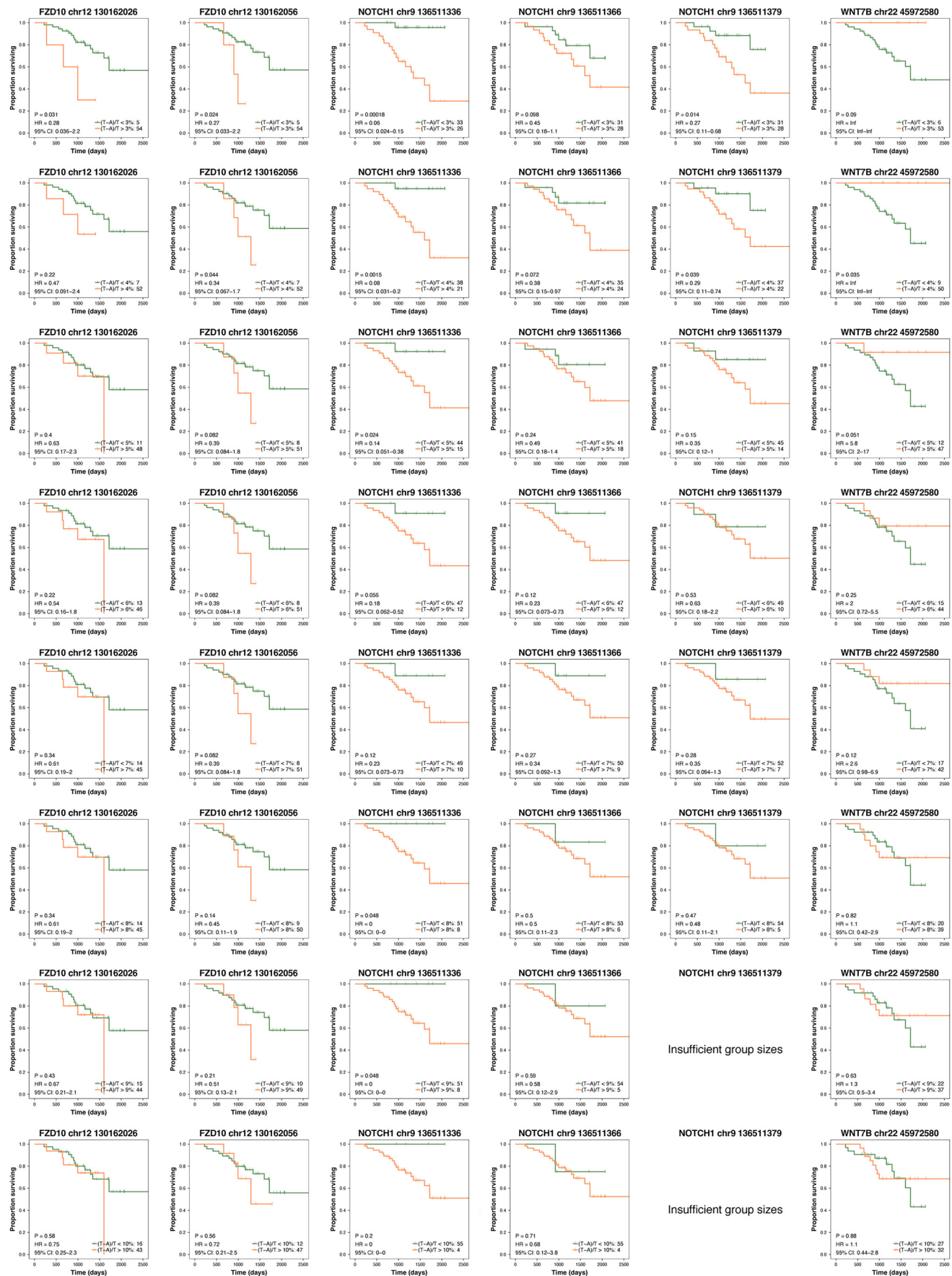




**Figure EV5. Kaplan-Meier survival curves illustrating the relationship between shallow DNA methylation changes at individual CpG sites and overall survival, using 3% to 10% methylation difference thresholds.**

*P* values of K-M survival analysis were calculated using chi-squared distribution.